Solar Phys (2011) 270: 297–310
DOI 10.1007/s11207-011-9753-2

Relationship between the Parameters of Coronal Holes and High-Speed Solar Wind Streams over an Activity Cycle

V.N. Obridko · B.D. Shelting

Received: 1 August 2010 / Accepted: 11 March 2011 / Published online: 14 April 2011

Abstract The comparison of the brightness and area of coronal holes (CH) to the solar wind speed, which was started by Obridko *et al.* (*Solar Phys.* **260**, 191, 2009a) has been continued. While the previous work was dealing with a relatively short time interval 2000 – 2006, here we have analyzed the data on coronal holes observed in the Sun throughout activity Cycle 23. A catalog of equatorial coronal holes has been compiled, and their brightness and area variations during the cycle have been analyzed. It is shown that CH is not merely an undisturbed zone between the active regions. The corona heating mechanism in CH seems to be essentially the same as in the regions of higher activity. The reduced brightness is the result of a specific structure with the magnetic field being quasi-radial at as low an altitude as $1.1 R_{\odot}$ or a bit higher. The plasma outflow decreases the measure of emission from CH. With an adequate choice of the photometric boundaries, the CH area and brightness indices display a fairly high correlation (0.6 – 0.8) with the solar wind velocity throughout the cycle, except for two years, which deviate dramatically – 2001 and 2007, *i.e.*, the maximum and the minimum of the cycle. The mean brightness of the darkest part of CH, where the field lines are nearly radial at low altitudes, is of the order of 18 – 20% of the solar brightness, while the brightness of the other parts of the CH is 30 – 40%. The solar wind streams originate at the base of the coronal hole, which acts as an ejecting nozzle. The solar wind parameters in CH are determined at the level where the field lines are radial.

Keywords Coronal hole · High-speed stream · Solar wind

1. Introduction

A systematic study of coronal holes began in 1973 – 1974, when detailed data were obtained from the *Skylab* mission (Zirker, 1977).

V.N. Obridko (✉) · B.D. Shelting
Pushkov Institute of Terrestrial Magnetism, Ionosphere, and Radio Wave Propagation (IZMIRAN), Russian Academy of Sciences, Troitsk, Russia
e-mail: obridko@izmiran.ru

Coronal holes usually occur in unipolar regions with the mainly open magnetic field. The high-speed solar wind (up to 1000 $\mathrm{km\,s^{-1}}$ at the Earth orbit) responsible for recurrent geomagnetic disturbances is closely linked up with coronal holes. The role of CH as the source of the high-speed solar wind streams (HSWS) was established in the early 1970s (Krieger, Timothy, and Roelof, 1973; Sheeley, Harvey, and Feldman, 1976; Kovalenko, 1983; Obridko *et al.*, 1986; Rozelot, 1983). A review of the physical conditions in coronal holes is given in Mogilevsky, Obridko, and Shilova (1997) and Obridko *et al.* (2009a, 2009b).

The basic concept of the solar wind states that the heliospheric magnetic field has an entirely solar origin and, by definition, originates in the open field regions (OFR) that occupy a relatively small part of the solar surface in the photosphere. The OFR distribution over the solar disk varies significantly, depending on the phase of the activity cycle. At the cycle minimum, the footpoints of the open field lines mainly are the regions around the solar poles. At the maximum, the OFR form narrow, isolated strips or cells.

The cycle of coronal holes can be described as follows. The change of sign of the polar field does not lead to immediate predominance of coronal holes of the "proper sign" for a given hemisphere. The background fields of old sign persist for a few years after the general reversal and vanish altogether only 4 – 5 years later (1 – 2 years before the cycle minimum). Then, 2 – 3 years after the minimum, numerous CHs of the new cycle appear again and, by the time of the new field reversal, the number of CHs of the old and new cycles become approximately equal.

At the end of the cycle minimum, when the activity begins to increase, narrow strips and patches of open field are formed from the polar region and move toward the equator. The polar domain of open fields breaks down, but it still persists until the beginning of the maximum epoch. During the maximum, the open field regions form narrow strips and curved corridors. At the end of the maximum, simply connected regions reappear, but they still do not cover the polar domain completely. The formation of a complete simply connected polar region of open fields marks the beginning of the minimum epoch.

Wang, Hawley, and Sheeley (1996) identified coronal holes with the open field regions and used the two terms interchangeably. But the full correspondence of these objects, including the correspondence of their boundaries, is virtually never observed. Besides, the very notion of a CH boundary is quite uncertain, depending both on the observing wavelength and on the assumed contrast at the boundary.

High-speed streams (HSS) are undoubtedly related to coronal holes and Source Surface (SS) IMF boundaries (Obridko and Shelting, 1987a, 1987b, 1989, 1990). Many authors analyzed the relationship between the CH magnetic field and solar wind velocity. Thus, Belov, Obridko, and Shelting (2006) obtained a high correlation between the magnetic field parameters in the Sun and the speed of the solar wind. The results of calculations with the modified flux–transport model (Wang and Sheeley, 1990, 1992; Arge and Pizzo, 2000) are available on the Internet site http://www.swpc.noaa.gov/ws/.

It is generally accepted that the magnetic field in coronal holes goes through "super-radial" expansion (Kovalenko, 1983; Wang and Sheeley, 1990; Wang, Sheeley, and Nash, 1990); *i.e.*, the field lines in these regions depart far from the radial direction, typical of magnetic monopole. The super-radial expansion begins at the base of the corona and reaches a factor of two at 1.4 solar radius ($R_\odot$) (Wang and Sheeley, 1990). This is due to the fact that the field lines everywhere on the source surface originate in the open field configurations connected with the coronal holes that cover only a small area in the lower corona and chromosphere.

Nolte *et al.* (1976) established a close relationship between the speed of the solar wind streams from a coronal hole and the area of the latter. Later on, the relationship between

CH area and HSS velocity was reported by various authors (Gosling and Pizzo, 1999; Zhang *et al.*, 2002, 2003; McComas and Elliot, 2002; Bromage, Browning, and Clegg, 2001; Veselovskii *et al.*, 2006; Robbins, Henney, and Harvey, 2006; Vršnak, Temmer, and Veronig, 2007a, 2007b). Since the brightness (contrast) of coronal holes depends on the divergence of the field lines, as also does the HSS velocity, one would expect a physical relation to exist between these quantities, which may be a reasonable parameter for predicting geophysical phenomena. It is fairly clear today that these zones are dominated by open magnetic field lines that act as efficient pipelines for transporting heated plasma from the corona into the solar wind. Because of this efficient transport mechanism, coronal holes have lower plasma density and, thus, they appear much darker than the quiet Sun (Cushman and Rense, 1976; Rottman, Orrall, and Klimchuk, 1982; Orrall, Rottman, and Klimchuk, 1983; Cranmer, 2001, 2002a, 2002b). Note that, unlike the regular corona, where the heat conduction loss is predominant, the loss in coronal holes is mainly determined by the solar wind stream (Withbroe and Noyes, 1977). The heat conduction at the base of the corona plays an important role in determining the mass loss rate in coronal holes (see, *e.g.*, Withbroe, 1988). There are some physical reasons to believe that the brightness (contrast) of CH must correlate with certain characteristics of the associated HSS, first of all with their velocity. This suggestion was made about ten years ago in Obridko (1998) and Obridko *et al.* (2000), but was not checked in experiments until lately (Luo *et al.*, 2008; Obridko *et al.*, 2009a, 2009b).

In view of the aforesaid, we have compared the CH pixel brightness over the time interval 2002 – 2006 with the solar wind speed (Obridko *et al.*, 2009a, 2009b). It was shown that the contrast of coronal holes determines the speed of the solar wind streams to the same extent as their area does. We analyzed more than 400 EUV images obtained by SOHO/EIT in the λ28.4 nm channel. The time interval under examination covered about 1500 days in the declining phase of Cycle 23 (from 2002 to 2006). We considered all coronal holes observed during that interval in the absence of coronal mass ejections (CME). Comparison was also made with some other parameters of the solar wind, such as density, temperature, and magnetic field. A fairly high correlation (0.70 – 0.89) was obtained with the velocity, especially during the periods of moderate activity. The brightness deficit in CH was found to be about 0.70 – 0.90 compared to the mean disk brightness on that day.

In that work, we only compared the CH contrast and solar wind velocity in the declining phase of solar activity. It is well known, however, that both the CH area and SW velocity change significantly with the cycle phase. The correlation between these parameters may change as well. So the objective of this work is to analyze the relationship between the parameters of coronal holes and associated high-speed streams over the entire Cycle 23.

2. Data and Calculation Methods

Hereinafter, we are using SOHO data in fits-format 1024 × 1024 in the 284 Å (28.4 nm) band downloaded from the Internet site http://umbra.nascom.nasa.gov/eit/eit-catalog.html treated with the Solarsoft program, which was downloaded from the site fttp://sohowww.nascom.nasa.gov/solarsoft/soho/eit/idl/anal/eit_prep.pro. A catalog of coronal holes was compiled for the period 1998 – 2009. For 1998 – 2002, the coronal holes were selected from *Solar Geophysical Data* by their configuration (simple oval shape far from other CH) and position on the disk (near the disk center). From 2003 to October 2009, the list of coronal holes was taken from the site "Coronal hole history" (since late October 2002) – http://www.dxlc.com/solar/coronal_holes.html. Our catalog includes all coronal holes that passed through the disk center unaccompanied by halo-type CME. The

data on the full-halo CME were taken from the catalogs in Gopalswamy *et al.* (2009) (http://cdaw.gsfc.nasa.gov/CME_list/HALO/halo.html). Our catalog comprises 338 coronal holes.

In our previous work, the solar wind velocity was taken at the instant when it reached its maximum value. Thus, the transport time was ignored. Here, we analyze correlation with the daily mean velocity V at transport times equal to three and four days. These data were downloaded from the Internet site http://nsssdc.gsfc.nasa.gov/omniweb/. The results based on the data at the peak velocity were compared with those obtained at a constant transport time. The difference proved to be of little importance when estimating the statistical relation between the CH parameters and SW velocity, though in some cases it may be significant. The comparison with the magnetic field structure was made using the WSO (John Wilcox Solar Observatory) data. The calculation method was described in the literature more than once (*e.g.*, see Hoeksema and Scherrer, 1986; Zhao, Hoeksema, and Scherrer, 1999; Obridko and Shelting, 1999a, 1999b). We have used the classical expansion coefficients; *i.e.*, the hypothesis of a radial field in the photosphere was not applied. All calculations were performed for 20 harmonics of the expansion.

In this work, like in Vršnak, Temmer, and Veronig (2007a, 2007b) and Obridko *et al.* (2009a, 2009b), the coronal holes have been considered at their passage through the central meridian. Vršnak, Temmer, and Veronig (2007a, 2007b) selected for this purpose the coronal holes in the meridional slices embracing the central meridian distance ranges $[-40°, -20°]$, $[-10°, 10°]$, and $[20°, 40°]$. In such a case, all coronal holes falling into this sector contribute to the calculated CH area and brightness. Obridko *et al.* (2009a) considered two geometric boundaries. One of them was also the meridional slice embracing the central meridian distance $[-10°, 10°]$. Besides, in order to eliminate the effect of the polar CHs, Obridko *et al.* (2009a) considered the coronal holes that fully or partly fell into the central circle of radius $0.6R_{\odot}$. This boundary passes at 36.9° of longitude and latitude and corresponds to the outer boundary in Vršnak, Temmer, and Veronig (2007a, 2007b). The position of these geometric boundaries is shown in Figure 1 in Obridko *et al.* (2009a). The analysis performed in that work showed that the correlation between the CH brightness and solar wind velocity somewhat increased after the polar CH had been eliminated. Therefore, we have used here only the coronal holes that were recorded within the central circle of radius $0.6R_{\odot}$, *i.e.*, did not fall beyond $\pm 36.9°$ (± 2.8 d) CMD. Henceforth, the CH area will be expressed in fractions of the area of this circle, which, in turn, makes 0.36 of the disk area.

The CH boundary inside this circle was determined with the aid of the additional photometric boundaries (see the next section).

We did not introduce correction for projection, and all areas were calculated in terms of the number of the pixels.

3. The Problem of CH Photometric Boundaries

When comparing the brightness and density of a coronal hole with the other characteristics, we meet with the problem of setting its boundaries. One can calculate the footpoints of the open field lines and compare them with CH images. This method was proposed by Scholl and Habbal (2008). However, a large number of the magnetic field harmonics ought to be calculated to give the inner fine structure of CH. Anyway, one can hardly expect the magnetic and inner photometric structure of CH to agree completely, since the latter depends not only on the magnetic structure but also on many other parameters of the solar plasma.

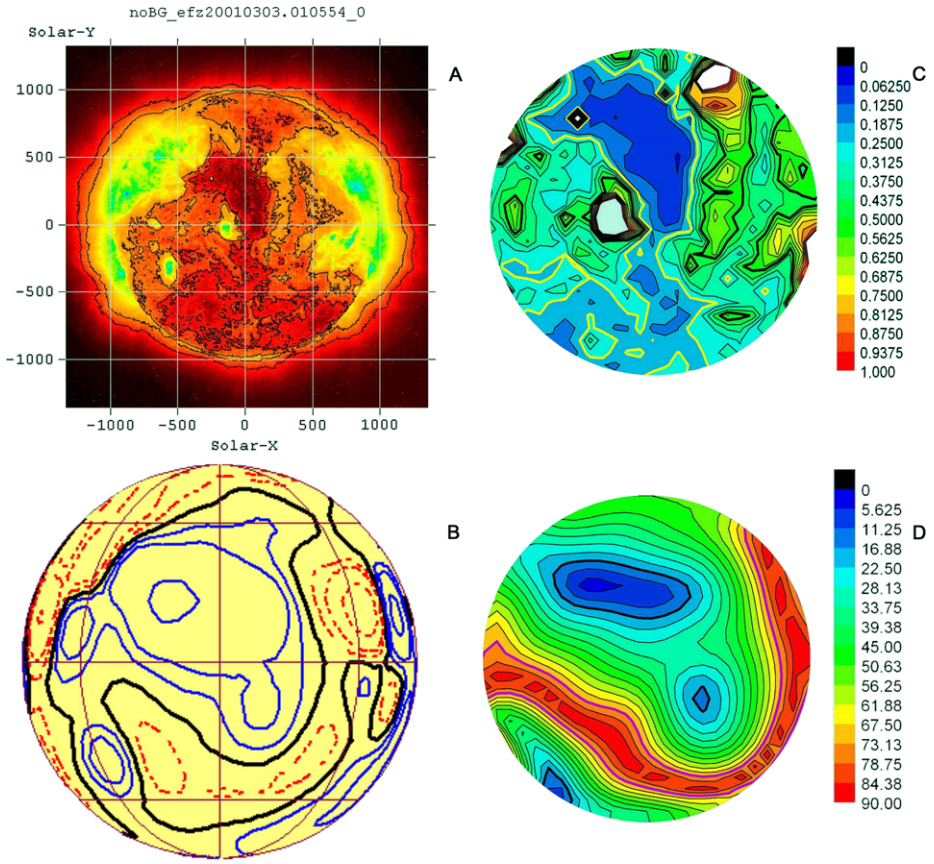

Figure 1 Comparison of the CH photometric and magnetic structure. Panel A displays the original SOHO/EIT image with the contour lines for RL = 4 and RL = 8; panel B shows the structure of the radial magnetic field at $1.1\,R_{\odot}$. The solid blue lines denote the positive polarity, and the dotted red ones the negative polarity. Panel C shows the brightness structure. The disks displayed in C and D correspond to the central disk of radius $0.6\,R_{\odot}$. The thick yellow line bounds the regions of 0.25 of the solar brightness and the thick black line, the regions of 0.5 of the solar brightness. Panel D shows the departure of the field lines from the radial direction at $1.1\,R_{\odot}$ in degrees; the thick black line corresponds to deviation $< 20^{\circ}$ from the radial direction, and the yellow line to deviation $< 75^{\circ}$.

Obridko *et al.* (2009a, 2009b), after a number of tests, assumed the standard value RL = 3 for the entire period 2002 – 2006. The CH contrast and areas calculated under this assumption displayed a high correlation with the solar wind velocity. So, this value is really adequate, at least for the time interval 2002 – 2004.

However, the standard constant RL turned out to be unacceptable when analyzing the CH contrast and area over a cycle. The standard RL suggests that the absolute brightness of CH is independent of the phase of the cycle. However, the CH brightness does change significantly from the maximum to the minimum. Therefore, we needed such a value of RL that would change during a cycle and could be determined objectively proceeding from the annual mean disk brightness. Test correlations with the solar wind velocity were calculated with RL determined as a share of the annual mean integral brightness. All values of the ratio of the CH mean brightness to the annual mean integral brightness of the disk in the range

of 0.1 – 1.0 were tried out at 0.1 steps. We failed to obtain unambiguous results; however, RL = 0.25 and RL = 0.5 of the corresponding annual mean disk brightness seemed to be the most appropriate values. As seen below, this choice proved to rest on sound physical grounds. The first value defines the darkest part of CH with radial field lines, and the second one the extended unipolar region.

4. Brightness and Magnetic Field Structure in CH

Eighteen coronal holes evenly distributed over all phases of Cycle 23 were selected to study the inner structure of CH. The results obtained are illustrated in Figure 1 using the 3 March 2001 coronal hole by way of example.

Figure 1a represents the original SOHO/EIT image with the contour lines for RL = 4 and RL = 8 that correspond, respectively, to the boundaries of 0.25 and 0.5 of the annual mean disk brightness in 2001. The figure was plotted using the standard FITS viewer package. One can see a very fine structure, tortuous isolines, and multiple dark inclusions inside a lighter zone, which give the impression of a blur. The darkest part is seen to lie within the first boundary (not necessarily at the center of the CH), while the second boundary encloses the entire hole. Figure 1b illustrates the structure of the radial magnetic field at $1.1\,R_{\odot}$. The solid blue lines denote positive polarity and the dotted red ones negative polarity. The brown latitude and longitude coordinate lines are plotted at a step of 45°. Figure 1c represents the brightness structure. For the sake of comparison with the magnetic field, a smoothing was performed at 0.5 heliographic degrees, and all brightness values were related to the annual mean disk brightness in 2001. The disk shown in the panel corresponds to the central disk of radius $0.6\,R_{\odot}$, *i.e.*, 36.9° (±2.8 d) CMD, and to the central part of Figures 1a and 1b. The thick yellow line bounds the regions of 0.25 of the solar brightness and the thick black line, the regions of 0.5 of the solar brightness. And finally, Figure 1d shows the departure of the field lines from the radial direction at $1.1\,R_{\odot}$ in degrees (this figure, too, was plotted only for the central disk of radius $0.6\,R_{\odot}$, *i.e.*, 36.9°). Here, the thick black line corresponds to deviation $< 20°$ from the radial direction and the yellow line, to deviation $< 75°$.

It is seen from the figure that:

- the darkest part of CH corresponds to the relative brightness less than 0.25 of the annual mean brightness of the solar disk;
- the CH as a whole corresponds to the relative brightness less than 0.5 of the annual mean disk brightness;
- the darkest part of CH corresponds to the maximum field strength at the given level;
- the darkest part of CH corresponds to the region where the departure from the radial direction is less than 20°;
- the CH as a whole is located in a unipolar field region;
- the field beyond the CH's darkest part can deviate from the radial direction significantly.

These properties are corroborated for all 18 coronal holes under examination and remind one of the structure of brightness and magnetic field in a sunspot consisting of the umbra and penumbra.

The index of unipolarity IU determined as the ratio of the absolute value of the mean radial magnetic field to its mean absolute value was calculated for control. We have

$$\mathrm{IU} = \left|\langle B_{\mathrm{R}}\rangle\right| \Big/ \langle |B_{\mathrm{R}}|\rangle.$$

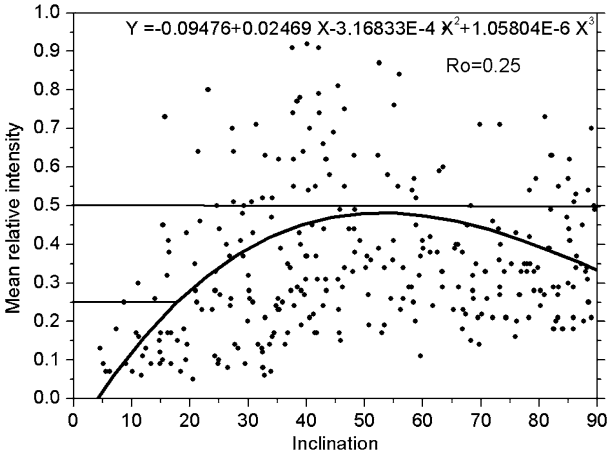

Figure 2 Correlation between the field line inclination to the normal and the relative brightness of coronal holes.

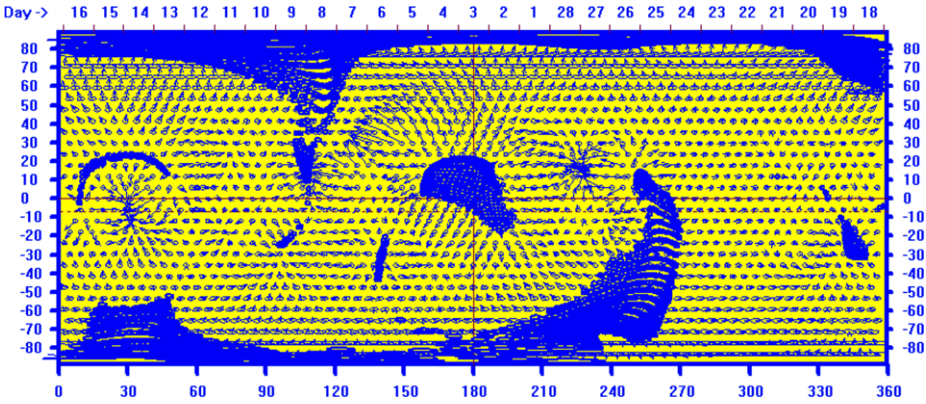

Figure 3 Synoptic map of the transverse magnetic field for a single rotation with the coronal hole of 3 March 2001 at the center. The blue circles mark the open field regions.

It is obvious that for a strictly unipolar field IU = 1.0, while for a multipolar region it will be close to zero. The index was calculated for all 338 coronal holes under examination. It turned out that at the altitude of $1.1\,R_{\odot}$, 281 holes (*i.e.*, 83%) had IU in the range of 0.9 – 1.0, and at $2.5\,R_{\odot}$ the number of such holes increased to 291 (86%). This agrees with the earlier result that the multipolarity of CH vanishes rapidly, and the hole becomes unipolar at as low an altitude as $1.05\,R_{\odot}$ (Stepanyan, 1995).

Figure 2 shows the relationship between the inclination of field lines to the normal and the relative brightness. In spite of a low correlation coefficient and a large spread of points, one can see that the relative brightness equal to 0.25 corresponds to an inclination angle of less than 18 – 20°, while the brightness of 0.50 corresponds to a strong inclination up to 50° or more.

Figure 3 represents a synoptic map of the transverse magnetic field at $1.1\,R_{\odot}$. The map is centered on 3 March 2001. The longitude of 180° (non-Carrington) on this synoptic map corresponds to the day of observation. On that day, a clearly pronounced coronal hole was observed at the center of the equatorial zone. The blue circles show the open field regions which agree closely with the darkest regions of the coronal hole. One can see the CH be-

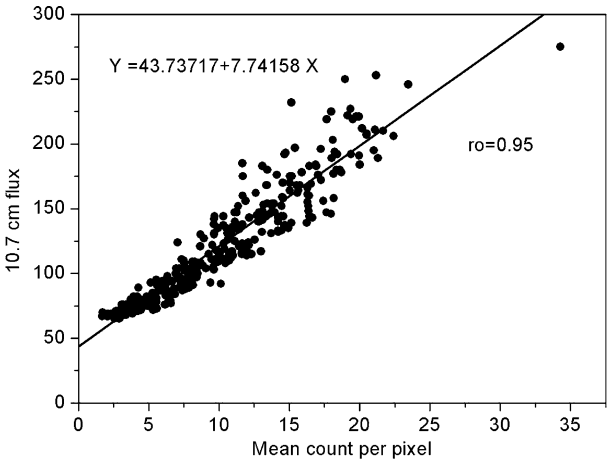

Figure 4 Comparison of the integral brightness of the Sun in the 28.4 nm band (SOHO/EIT), correlated with the 10-cm solar radio flux, taken from http://www.ngdc.noaa.gov/stp/solar/flux.html.

ing surrounded on all sides by divergent field lines. The structure resembles strongly the magnetic field in a sunspot (Mogilevsky, Obridko, and Shilova, 1997).

Thus, we arrive at the conclusion that the level at which the field lines in a coronal hole become radial corresponds to the darkest part of the hole at $1.1R_{\odot}$ or somewhat higher. Outside the darkest region, the divergence of the field lines increases, and at the source surface, they come to fill the unipolar zone completely. The field lines are radial throughout the source surface (in our case, at $2.5R_{\odot}$), but over the darkest part of the coronal hole they become radial at much lower altitudes.

5. Variation of CH Relative Brightness and Area over Cycle 23

5.1. Comparison with Radio Emission

Obridko *et al.* (2009a) compared the mean brightness of the corona at 28.4 nm with the solar brightness in the 10.7 cm radio range. The 10.7 cm solar radio emission is generated at the temperature of 10^5 K, while the radiation at 28.4 nm corresponds to much higher temperatures, 2×10^6 K. Besides, these two types of radiation occur at different heights in the corona, at different densities and magnetic field values, and they are generated by different mechanisms. Therefore, it should not be surprising if they were not related at all. However, they proved to display a correlation as high as 0.90. Only for very high and very low values the correlation is not quite linear.

However, this comparison was based on the data for the period 2002 – 2006, *i.e.*, for the epoch of high solar activity. It was not clear whether the correlation revealed would hold all over the cycle. In this work, we have constructed a scatter-plot diagram (see Figure 4) based on the data for 338 days selected earlier over the entire Cycle 23 and included in our catalog. Instead of having disappeared, the correlation became even higher, the correlation coefficient amounting to 0.95 ± 0.005. This suggests that the coronal heating mechanisms are universal both all over the disk and in the coronal holes, at least in the equatorial zone. And though the corona brightness depends strongly on the phase of the cycle, the correlation between different emissions remains constant.

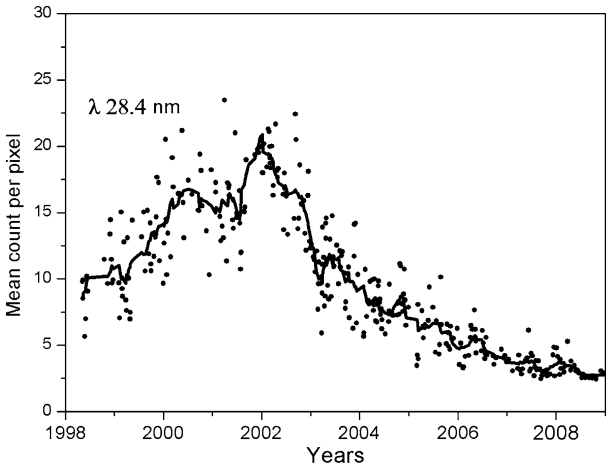

Figure 5 Mean brightness of the Sun at the wavelength of 28.4 nm as a function of time.

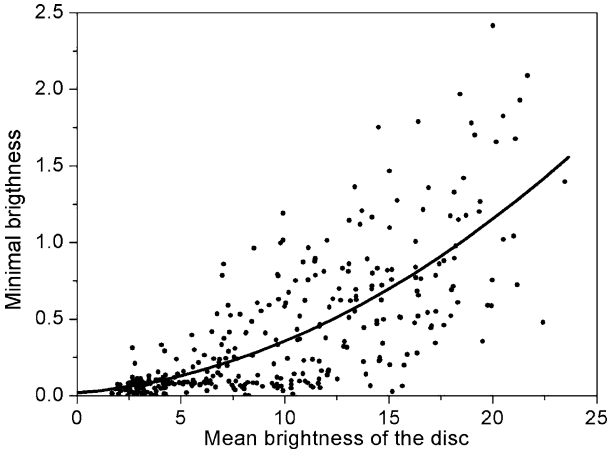

Figure 6 Comparison of the minimum brightness in each CH with the mean disk brightness on the given day as observed in 28.4 nm in the period of 1998–2008.

5.2. CH Relative Brightness

Figure 5 shows the variation of the mean brightness of the Sun at the 28.4 nm wavelength as defined by the per pixel count rate. One can see that the brightness changes significantly with the phase of the cycle. At the peak of the curve, which falls on 2002 (*i.e.* two years after the calendar date of the cycle maximum), the brightness reaches 22 counts per pixel. At the minimum, it is ten times lower.

We have calculated the mean brightness of coronal holes (annual mean number of counts per pixel) over the entire disk and in the central zone (over a disk of radius $0.6R_{\odot}$) with the photometric boundary at two reference levels (RL) – RL = 0.25 and RL = 0.50 of the mean disk brightness for the given year;

It turned out that the cycle dependence of CH brightness is virtually a replica of the behavior of the disk brightness as a whole. This means that the mechanisms that control the EUV brightness of the solar atmosphere work also in CH. Thus, coronal holes are not just gaps between active regions, and the traditional heating mechanisms are likely to work there, too. However, the matter outflow along the open field lines decreases the effective emission measure (Obridko *et al.*, 2009a, 2009b).

The question naturally arises whether the similarity of time variations of the brightness in CH and the mean disk brightness is merely the result of our definition of the photometric boundaries. Of course, we calculate the mean brightness within the photometric boundaries, and a complete similarity is only possible if the brightness distribution in individual pixels is equal for all CH. Still doubt remains, and as a check we have compared the minimum brightness in each hole with the mean disk brightness on the given day. The minimum CH brightness has nothing to do with the photometric boundary and does not depend on any assumptions. Figure 6 illustrates the dependence of the minimum brightness on the mean disk brightness. One can see that the former does increase with the increase of the latter. The linear correlation coefficient is 0.728 ± 0.025. The figure represents also a second-order fitting curve for which the correlation coefficient is somewhat higher (0.742).

Sure enough, the brightness of small holes in the vicinity of the sunspot maximum may be contaminated by scattering from the nearby active regions. This is difficult to take into account. For the sake of control, we have found here, the same as in our previous work, the minimum brightness in the coronal hole. This value usually behaves like the CH mean contrast.

Another factor that might have affected our correlations is that the EIT 28.4 nm bandpass is heavily blended with cool emission lines like Si VII 27.5 nm (see, *e.g.*, Del Zanna, Bromage, and Mason, 2003). The EIT 19.5 nm band[1] would be more convenient for this analysis. However, since this paper is an extension of our previous study (Obridko *et al.*, 2009a) to a vaster database, we preferred not to change the bandpass. The preliminary analysis we made for the EIT 19.5 nm band did not change the results significantly and will be published separately.

5.3. Variations in the CH Relative Area

Figure 7 illustrates variations in the relative CH area in the central zone of the Sun (which lies inside a circle of radius $0.6 R_\odot$ and occupies 0.36 of the total disk area) at two values of the photometric boundary: RL = 0.25 of the total annual mean brightness (squares) and RL = 0.50 (circles).

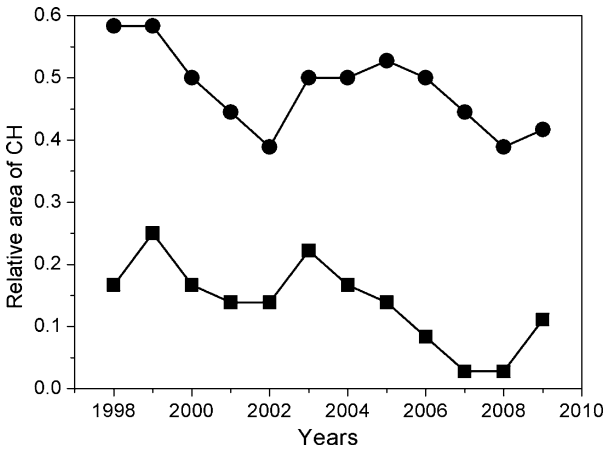

Figure 7 Variation of CH area relative to the area of the central circle for two values of the photometric boundary as a function of time. The circles and squares correspond to the photometric boundary at 0.5 and 0.25 of the mean disk brightness, respectively.

[1]The authors are grateful for this remark to the reviewer, as well as to V. Grechnev and V. Slemzin.

One can see that the relative area of the central holes decreases at the maximum of the cycle whatever photometric boundary is chosen. The relative brightness is maximal at the rise and decline of the activity cycle.

At the minimum of Cycle 23, coronal holes are observed mainly at the poles. In the central part of the disk, they are few and have small areas.

6. Comparison with the Solar Wind Velocity

In our previous work, we compared the CH parameters with the solar wind velocity using the indices of area and contrast. The solar wind velocity itself changes chaotically without displaying any systematic regularity.

Since it was not *a priori* clear which CH indices would be most convenient for estimating the correlation with the solar wind velocity, we have used the photometric boundary at two levels:

i) CH area and mean brightness at RL = 0.25 of the annual mean brightness and
ii) CH area and mean brightness at RL = 0.50 of the annual mean disk brightness.

As follows from the previous section, the first boundary outlines the darkest part of CH, while the second one bounds its lighter part, which fills the entire unipolar region.

It turned out that the best correlation with the solar wind velocity was obtained for the area of the "umbra" and the overall mean brightness of CH including "penumbra".

Figure 8 illustrates how the correlation between CH indices and the solar wind velocity varies at a transport time of four days. The black squares show the correlation with the area of the darkest part and the red circles the correlation with the mean brightness of the coronal hole. Since the correlation with the area is positive and with the brightness it is negative, we give the absolute values of the correlation coefficient.

Lately, Luo *et al.* (2008) calculated the solar wind velocity at the Earth from CH brightness in the channel λ28.4 nm and obtained quite a high correlation for a relatively short time interval from November 21 to December 26 2003. It should be noted, however, that the prognostic index they used was not the CH brightness *per se* but the inverse brightness in each pixel averaged over a particular circle at the center of the Sun. This value may differ significantly from the mean brightness. This is difficult to interpret physically, since in

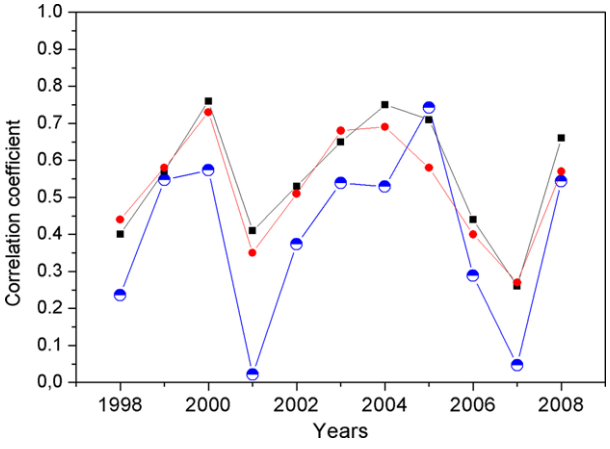

Figure 8 Correlation between CH indices and solar wind velocity. The black squares, red circles, and half-filled circles show the correlation with the area of the darkest part, mean CH brightness, and the Luo index (Luo *et al.*, 2008), respectively.

all heating and energy transport mechanisms we are dealing with the brightness rather than its inverse value. Besides, the relative error increases, because very small brightness values enter in the Luo index with a large weight. The half-filled circles in Figure 8 show the correlation with the Luo index (Luo *et al.*, 2008). It is readily seen that the Luo index is nowhere better than our indices. On the contrary, in most cases it yields lower correlation. The only point at which the correlation with the Luo index is close to ours is 2005 – the year for which it was first introduced.

It is interesting to note that all three indices, though determined in quite different ways, yield a similar time dependence of the correlation coefficient.

Thus, the indices we have proposed display a high correlation (0.6 – 0.8) with the solar wind velocity. However, two years (2001 and 2007) deviate from the general behavior. As for 2001, such a result ought to be expected. This was the epoch of the maximum of Cycle 23, when the disk brightness at 28.4 nm was very large (Figure 6) and the area of equatorial coronal holes was very small (Figure 7). The 2001 minimum is well pronounced on the curve and is corroborated by two independent studies. The decrease of correlation between the CH area and solar wind velocity in 2001 was also found by Veselovsky *et al.* (2006). Robbins, Henney, and Harvey (2006) showed the correlation between the solar wind velocity and CH area to decrease in the epochs of high solar activity. Thus, the general tendency for the fast wind to come from the darker parts of coronal holes is sometimes violated.

7. Conclusions

In this work, we have analyzed the data on coronal holes recorded throughout the activity Cycle 23. A catalog was compiled that comprises 338 coronal holes observed in the central disk of the Sun ($R < 0.6 R_{\odot}$) in the absence of the halo-type coronal mass ejections.

The cycle variations in CH brightness and area have been investigated. It turned out that the cycle dependence of CH brightness was virtually a replica of the behavior of the disk brightness as a whole and was part of the general cyclic variation in the mean brightness of the Sun. This might be considered to be merely an effect of the choice of the photometric boundary. However, a direct comparison of the minimum brightness in coronal holes with the mean disk brightness on the given day reveals a correlation with a coefficient 0.742, which agrees with the result obtained by Badalyan (1995) from the analysis of data of 16 total solar eclipses for the period 1952 – 1983. According to her calculations, the density in equatorial coronal holes increases by a factor of 1.5 – 2 as we approach the maximum of the activity cycle. The temperature also increases at the maximum by approximately 20 – 25% in the polar CH, and somewhat less in the equatorial ones.

Thus, coronal holes are not just undisturbed areas between the active regions. The coronal heating mechanisms in equatorial CHs seem to be the same as in the more active regions. Their decreased brightness is due to a specific structure with quasi-radial magnetic field at a level as low as $1.1 R_{\odot}$ or somewhat higher. The matter outflow decreases the CH emission measure.

As shown earlier in Badalyan and Obridko (2006, 2007), two regularities observed in the relationship between the magnetic field and green-line coronal brightness can be explained by a different relative contributions of the heating mechanisms, depending on the observation latitude. The models based on slow dissipation of the field (DC) are more efficient in the equatorial zone and the wave models based on dissipation of Alfvén waves (AC), in the polar zone.

With appropriately chosen values of the photometric boundary, the CH area and brightness indices display a fairly high correlation (0.6 – 0.8) with the solar wind velocity throughout the cycle except for two years – 2001 and 2007, *i.e.*, the maximum and minimum of the cycle, which deviate dramatically.

Not only do the open magnetic fields determine the very existence of coronal holes, but their structure determines the inner structure of CH. The main factors are, obviously, the field intensity and the divergence of the field lines. A combination of these factors is responsible for the complex inner structure of CH. The mean brightness of the darkest part of CH corresponds to the region where the angle of the magnetic field with the normal does not exceed 15 – 20°. Here, the brightness is less than 25% of the mean solar brightness and comprises 18 – 20%. In the outer CH regions, where the angle of the field line with the normal does not exceed 50°, the mean brightness amounts to 30 – 40%.

We adopted a scheme similar to that proposed by Wang, Kundu, and Yoshimura (1988) to account for radio observations of CH and confirmed in later work (Mogilevsky, Obridko, and Shilova, 1997; Obridko, 1998).

The high-speed stream forms entirely at the base of the coronal hole. The parameters of the solar wind are determined at the level where the field lines in CH are radial. So, the final wind speed is determined by the flux-tube expansion rate at the base of the corona (as in Wang and Sheeley, 1990). The coronal hole acts as a nozzle out of which the stream is ejected.

Acknowledgements The work was sponsored by the Russian Foundation for Basic Research, Project No. 08-02-00070. We are grateful to the SOHO team and SWO for the data we have used in our study.

References

Arge, C.N., Pizzo, V.J.: 2000, *J. Geophys. Res.* **105**, 10465.
Badalyan, O.G.: 1995, *Astron. Astrophys. Trans.* **9**, 205.
Badalyan, O.G., Obridko, V.N.: 2006, *Solar Phys.* **238**, 271.
Badalyan, O.G., Obridko, V.N.: 2007, *Astron. Lett.* **33**, 182.
Belov, A.V., Obridko, V.N., Shelting, B.D.: 2006, *Geomagn. Aeron.* **46**, 430.
Bromage, B.J.I., Browning, P.K., Clegg, J.R.: 2001, *Space Sci. Rev.* **97**, 13.
Cranmer, S.R.: 2001, Coronal holes. In: Murdin, P. (ed.) *Encyclopedia of Astronomy and Astrophysics*. Inst. of Phys., Bristol, article 1999.
Cranmer, S.R.: 2002a, *COSPAR Coll. Ser.* **13**, 3.
Cranmer, S.R.: 2002b, *Space Sci. Rev.* **101**, 229.
Cushman, G.W., Rense, W.A.: 1976, *Astrophys. J. Lett.* **207**, 61.
Del Zanna, G., Bromage, B.J.I., Mason, H.E.: 2003, *Astron. Astrophys.* **398**, 743.
Gosling, J.T., Pizzo, V.J.: 1999, *Space Sci. Rev.* **89**, 21.
Gopalswamy, N., Yashiro, S., Michalek, G., Stenborg, G., Vourlidas, A., Freeland, S., Howard, R.: 2009, *Earth Moon Planets* **104**, 295.
Hoeksema, J.T., Scherrer, P.H.: 1986, *The solar magnetic field – 1976-through 1985.* Report UAG-94, WDC-A for Solar Terrestrial Physics.
Kovalenko, V.A.: 1983, *Solar Wind*, Nauka, Moscow, 3 – 271.
Krieger, A.S., Timothy, A.F., Roelof, E.C.: 1973, *Solar Phys.* **29**, 505.
Luo, B., Zhong, Q., Liu, S., Gong, J.: 2008, *Solar Phys.* **250**, 159.
McComas, D.J., Elliot, H.A.: 2002, *Geophys. Res. Lett.* **29**, 1314.
Mogilevsky, E.I., Obridko, V.N., Shilova, N.S.: 1997, *Solar Phys.* **176**, 107.
Nolte, J.T., Krieger, A.S., Timothy, A.F., Gold, R.E., Roelof, E.C., Vaiana, G., Lazarus, A.J., Sullivan, J.D., McIntosh, P.S.: 1976, *Solar Phys.* **46**, 303.
Obridko, V.N.: 1998, In: Feng, X.H., Wei, F.S., Dryer, M. (eds.) *Advances in Solar Connection with Transient Interplanetary Phenomena, Proc. Third SOLTIP Symp*, International Academic Publishers, Beijing, 41.
Obridko, V.N., Shelting, B.D.: 1987a, *Geomagn. Aeron.* **27**, 197.
Obridko, V.N., Shelting, B.D.: 1987b, *Geomagn. Aeron.* **27**, 660.

Obridko, V.N., Shelting, B.D.: 1989, *Solar Phys.* **124**, 73.
Obridko, V.N., Shelting, B.D.: 1990, *Astron. Zh.* **67**, 890.
Obridko, V.N., Shelting, B.D.: 1999a, *Solar Phys.* **187**, 185.
Obridko, V.N., Shelting, B.D.: 1999b, *Solar Phys.* **184**, 187.
Obridko, V.N., Konstantinova, L.Yu., Konakh, M.M., Mansurov, G.S.: 1986, *Geomagn. Aeron.* **26**, 313.
Obridko, V.N., Fomichev, V.V., Kharshiladze, A.F., Zhitnik, I., Slemzin, V., Wu, S.W., Ding, J., Hathaway, D.: 2000, *Astron. Astrophys. Trans.* **18**, 819.
Obridko, V.N., Shelting, B.D., Livshits, I.M., Asgarov, A.B.: 2009a, *Solar Phys.* **260**, 191.
Obridko, V.N., Shelting, B.D., Livshits, I.M., Askerov, A.B.: 2009b, *Astron. Rep.* **53**, 1050.
Orrall, F.Q., Rottman, G.J., Klimchuk, J.A.: 1983, *Astrophys. J. Lett.* **266**, 65.
Robbins, S., Henney, C.J., Harvey, J.W.: 2006, *Solar Phys.* **233**, 265.
Rottman, G.J., Orrall, F.Q., Klimchuk, J.A.: 1982, *Astrophys. J.* **260**, 326.
Rozelot, J.P.: 1983, *Ann. Phys.* **8**, 539.
Scholl, I.S., Habbal, S.R.: 2008, *Solar Phys.* **248**, 425.
Sheeley, N.R. Jr., Harvey, J.W., Feldman, W.C.: 1976, *Solar Phys.* **49**, 271.
Stepanyan, N.N.: 1995, *Izv. RAN Phys. Ser.* **59**, 63.
Veselovskii, I.S., Persiantsev, I.G., Rusanov, A.Yu., Shugai, Yu.S.: 2006, *Astron. Vestn.* **40**, 427 [*Solar Syst. Res.* **40**, 427 (2006)].
Vršnak, B., Temmer, M., Veronig, A.M.: 2007a, *Solar Phys.* **240**, 315.
Vršnak, B., Temmer, M., Veronig, A.M.: 2007b, *Solar Phys.* **240**, 331.
Wang, Y.-M., Sheeley, N.R. Jr.: 1990, *Astrophys. J.* **355**, 726.
Wang, Y.-M., Sheeley, N.R. Jr.: 1992, *Astrophys. J.* **392**, 310.
Wang, Y.-M., Sheeley, N.R. Jr., Nash, A.G.,: 1990, *Nature* **347**, 439.
Wang, Y.-M., Hawley, S.H., Sheeley, N.R. Jr.: 1996, *Science* **271**, 464.
Wang, Z., Kundu, M.R., Yoshimura, H.: 1988, In: *Solar and Stellar Coronal Structure and Dynamics, Proc. of the Ninth Sacramento Peak Summer Symp.*, *Sunspot, NM*, *Aug. 17 – 21, 1987*. National Solar Observatory, Sunspot, 458 (A89-20526 06-92).
Withbroe, G.L.: 1988, *Astrophys. J.* **325**, 442.
Withbroe, G.L., Noyes, R.W.: 1977, In: *Annu. Rev. Astron. Astrophys.* **15**, Annual Rewievs, Inc., Palo Alto, 363 (A78-16576 04-90).
Zhang, J., Woch, J., Solanki, S.K., von Steiger, R.: 2002, *Geophys. Res. Lett.* **29**, 1236.
Zhang, J., Woch, J., Solanki, von Steiger, R., Forsyth, R.: 2003, *J. Geophys. Res.* **108**, 1144.
Zhao, X.P., Hoeksema, J.T., Scherrer, P.H.: 1999, *J. Geophys. Res.* **104**, 9735.
Zirker, J.B.: 1977, In: Zirker, J.B. (ed.) *Coronal Holes and High Speed Wind Streams, Skylab Solar Workshop*, Colorado Assoc. Univ. Press, Denver, 1.